Title
Tau pathology and neurodegeneration contribute to cognitive impairment in Alzheimer's disease

Journal
Brain, 140(12)

ISSN
0006-8950

Authors
Bejanin, Alexandre
Schonhaut, Daniel R
La Joie, Renaud
et al.

Publication Date
2017-12-01

DOI
10.1093/brain/awx243

Peer reviewed

doi:10.1093/brain/awx243 BRAIN 2017: 140; 3286–3300 | 3286

BRAIN
A JOURNAL OF NEUROLOGY

Tau pathology and neurodegeneration contribute to cognitive impairment in Alzheimer's disease

Alexandre Bejanin,[1] Daniel R. Schonhaut,[1] Renaud La Joie,[1] Joel H. Kramer,[1] Suzanne L. Baker,[2] Natasha Sosa,[1] Nagehan Ayakta,[1] Averill Cantwell,[1] Mustafa Janabi,[2] Mariella Lauriola,[1] James P. O'Neil,[2] Maria L. Gorno-Tempini,[1] Zachary A. Miller,[1] Howard J. Rosen,[1] Bruce L. Miller,[1] William J. Jagust[2,3] and Gil D. Rabinovici[1,2,3]

Neuropathological and *in vivo* studies have revealed a tight relationship between tau pathology and cognitive impairment across the Alzheimer's disease spectrum. However, tau pathology is also intimately associated with neurodegeneration and amyloid pathology. The aim of the present study was therefore to assess whether grey matter atrophy and amyloid pathology contribute to the relationship between tau pathology, as measured with ^{18}F-AV-1451-PET imaging, and cognitive deficits in Alzheimer's disease. We included 40 amyloid-positive patients meeting criteria for mild cognitive impairment due to Alzheimer's disease ($n = 5$) or probable Alzheimer's disease dementia ($n = 35$). Twelve patients additionally fulfilled the diagnostic criteria for posterior cortical atrophy and eight for logopenic variant primary progressive aphasia. All participants underwent 3 T magnetic resonance imaging, amyloid (^{11}C-PiB) positron emission tomography and tau (^{18}F-AV-1451) positron emission tomography, and episodic and semantic memory, language, executive and visuospatial functions assessment. Raw cognitive scores were converted to age-adjusted Z-scores (W-scores) and averaged to compute composite scores for each cognitive domain. Independent regressions were performed between ^{18}F-AV-1451 binding and each cognitive domain, and we used the Biological Parametric Mapping toolbox to further control for local grey matter volumes, ^{11}C-PiB uptake, or both. Partial correlations and causal mediation analyses (mediation R package) were then performed in brain regions showing an association between cognition and both ^{18}F-AV-1451 uptake and grey matter volume. Our results showed that decreased cognitive performance in each domain was related to increased ^{18}F-AV-1451 binding in specific brain regions conforming to established brain-behaviour relationships (i.e. episodic memory: medial temporal lobe and angular gyrus; semantic memory: left anterior temporal regions; language: left posterior superior temporal lobe and supramarginal gyrus; executive functions: bilateral frontoparietal regions; visuospatial functions: right more than left occipitotemporal regions). This pattern of regional associations remained essentially unchanged—although less spatially extended—when grey matter volume or ^{11}C-PiB uptake maps were added as covariates. Mediation analyses revealed both direct and grey matter-mediated effects of ^{18}F-AV-1451 uptake on cognitive performance. Together, these results show that tau pathology is related in a region-specific manner to cognitive impairment in Alzheimer's disease. These regional relationships are weakly related to amyloid burden, but are in part mediated by grey matter volumes. This suggests that tau pathology may lead to cognitive deficits through a variety of mechanisms, including, but not restricted to, grey matter loss. These results might have implications for future therapeutic trials targeting tau pathology.

1 Memory and Aging Center, University of California San Francisco, San Francisco, CA, USA
2 Molecular Biophysics and Integrated Bioimaging Division, Lawrence Berkeley National Laboratory, Berkeley, CA, USA
3 Helen Wills Neuroscience Institute, University of California Berkeley, Berkeley, CA, USA

Received April 8, 2017. Revised July 3, 2017. Accepted August 3, 2017. Advance Access publication October 7, 2017

Correspondence to: Alexandre Bejanin
University of California, San Francisco (UCSF)
Memory and Aging Center MC: 1207
675 Nelson Rising Lane, Suite 190
San Francisco, CA 94158, USA
E-mail: bejanin@cyceron.fr

Keywords: Alzheimer's disease; tau; amyloid; atrophy; cognitive impairment

Abbreviations: DVR = distribution volume ratio; MCI = mild cognitive impairment; NFT = neurofibrillary tangle; SUVR = standard uptake value ratio

Introduction

Alzheimer's disease is a dual proteinopathy characterized by extracellular deposits of fibrillar amyloid-β peptides and aggregates of the phosphorylated microtubule-associated protein tau in neurofibrillary tangles (NFTs; Hyman *et al.*, 2012). Growing evidence suggests that both amyloid-β and tau proteins accumulate and spread years before the development of clinical symptoms (Braak and Del Tredici, 2015), raising questions about their specific and common contribution to cognitive impairment.

Pioneering neuropathological studies showed that the burden of NFTs, but not of amyloid-β plaques, correlates with the degree of cognitive impairment in Alzheimer's disease (Arriagada *et al.*, 1992*a*) and non-demented elderly individuals (Arriagada *et al.*, 1992*b*). Further clinicopathological studies reported that not only the density, but also the extent of NFTs, are associated with ante-mortem cognitive status (Nelson *et al.*, 2012). These results have been recently replicated by *in vivo* studies using PET radiotracers binding to NFTs, such as ^{18}F-AV-1451, and showing that more advanced Braak stages are associated with decreased global cognitive status and more frequent cognitive impairment (Cho *et al.*, 2016*a*; Schöll *et al.*, 2016). The neuroanatomic distribution of tau pathology also correlates with specific cognitive domain performance. Hence, medial temporal lobe NFTs (Mitchell *et al.*, 2002; Guillozet *et al.*, 2003) and ^{18}F-AV-1451 uptake (Ossenkoppele *et al.*, 2016; Schöll *et al.*, 2016) have been related to episodic memory, but not to other cognitive functions, in cognitively normal older adults and subjects with cognitive impairment. Finally, both post-mortem (Hof *et al.*, 1989; Murray *et al.*, 2011; Gefen *et al.*, 2012) and *in vivo* (Dronse *et al.*, 2016; Ossenkoppele *et al.*, 2016) studies revealed that the spatial distribution of tau pathology is closely linked to the clinical phenotype in Alzheimer's disease dementia.

Together, these results suggest a close relationship between NFTs and cognitive impairment across the Alzheimer's disease spectrum. In contrast, amyloid-β pathology has only a relatively modest direct correlation with cognition (Nelson *et al.*, 2012). Indeed, most studies have reported either absent or weak association between regional amyloid-β plaques and specific cognitive impairment in Alzheimer's disease patients (Arriagada *et al.*, 1992*a*; Guillozet *et al.*, 2003) and the reduction of plaque load in the brain in therapeutic trials has not thus far yielded cognitive benefit in Alzheimer's disease patients (Salloway *et al.*, 2014). This discrepancy might be explained by the fact that, as compared to amyloid-β plaques, tau pathology is more intimately related to neuronal loss (Gómez-Isla *et al.*, 1997; Giannakopoulos *et al.*, 2003). Indeed, NFTs appear to parallel grey matter atrophy (Jack *et al.*, 2002; Whitwell *et al.*, 2008), which in turn has been extensively associated with cognitive impairment. It is therefore possible that the impact of tau pathology on cognition is mediated by grey matter loss. Using ^{18}F-AV-1451-PET imaging, we aimed at assessing this specific question in a heterogeneous sample of Alzheimer's disease patients. Specifically, our objective was to assess the specific relationships between cognitive impairment and tau pathology and to test if these relationships remained significant after controlling for local grey matter atrophy and amyloid pathology. We also performed causal mediation analyses to further examine the intermediary role of grey matter atrophy in the relationship between ^{18}F-AV-1451 and cognitive deficits.

Materials and methods

Participants

Forty patients were recruited from the University of California San Francisco (UCSF) Alzheimer's Disease Research Center (Table 1 for demographic data). A subset of these patients was included in previous publications from our laboratory (Ossenkoppele *et al.*, 2016; Schöll *et al.*, 2016). All patients received a standard clinical evaluation that included a comprehensive neurological history, physical and neurological examinations, structured caregiver interviews, brain MRI and neuropsychological testing. Clinical diagnosis was established by consensus in a multidisciplinary team. All participants met clinical criteria for probable Alzheimer's disease dementia ($n = 35$; McKhann *et al.*, 2011) or mild cognitive impairment (MCI) due to Alzheimer's disease ($n = 5$; Albert *et al.*, 2011). Twelve patients additionally met diagnostic criteria for posterior cortical atrophy (Mendez *et al.*, 2002) and eight for logopenic variant primary progressive aphasia (Gorno-Tempini *et al.*, 2011), now recognized as visual and language-predominant phenotypes of Alzheimer's disease (McKhann *et al.*, 2011; Dubois *et al.*, 2014). Several patients who met McKhann *et al.* (2011) criteria for probable Alzheimer's

Table 1 Demographic and neuropsychological data for the overall population and within each clinical subgroup

	All patients	AD	lvPPA	PCA	MCI	*P*-values
Gender (male/female)	17/23	7/8	2/6	6/6	2/3	*NA*
Age (years)	62.9 ± 8.4	64 ± 9.1	63.3 ± 8.3	61.9 ± 7.5	61.6 ± 10.3	*P* = 0.901
Education[e] (years)	17.5 ± 3	17.2 ± 2.8	17.8 ± 1.8	16.8 ± 3.7	19.6 ± 2.6	*P* = 0.167
Amyloid PET (PiB) Pos/Neg	40/0	15/0	8/0	12/0	5/0	*NA*
APOE ε2/ε3, ε2/ε4, ε3/ε3, ε3/ε4, ε4/ε4	1, 2, 19, 15, 3	0, 1, 7, 6, 1	0, 1, 5, 2, 0	0, 0, 6, 5, 1	1, 0, 1, 2, 1	*NA*
MMSE[f] (/30)	22.2 ± 5.8	20.6 ± 5.1	22.1 ± 6.9	21.5 ± 5.6	28.6 ± 1.5	***P* = 0.012**[a]
CDR - Sum of Boxes[g] (/18)	3.8 ± 2.3	4.4 ± 1.3	3 ± 2.4	4.7 ± 3	1.9 ± 0.8	***P* = 0.034**[b]
Episodic Memory (W-score)	−2.7 ± 1.5	−3.2 ± 0.8	−2.5 ± 1.8	−3 ± 1.3	−0.6 ± 1.2	***P* = 0.021**[b]
Semantic Memory[f] (W-score)	−1.9 ± 1.8	−1.5 ± 1.6	−2.9 ± 2.4	−2.3 ± 1.3	−0.1 ± 0.3	***P* = 0.006**[a]
Language[f] (W-score)	−1.6 ± 1.8	−0.8 ± 0.8	−3.1 ± 1	−2.3 ± 2.4	−0.1 ± 1	***P* = 0.002**[c]
Executive functions (W-score)	−2.2 ± 1.1	−2.3 ± 1	−2.5 ± 0.9	−2.6 ± 0.9	−0.4 ± 0.5	***P* = 0.005**[a]
Visuospatial functions[f] (W-score)	−3 ± 3.9	−1.7 ± 2.2	−1.8 ± 4	−7.1 ± 3.8	0 ± 0.7	***P* = 0.002**[d]
Interval MRI-Neuropsychological exam (days)	27.2 ± 67.1	37.3 ± 52.3	54.4 ± 131.1	6.7 ± 11.3	2.8 ± 4.7	*P* = 0.858
Interval AV-1451-Neuropsychological exam (days)	77.4 ± 76.7	107.2 ± 87.8	80.3 ± 58.9	57.8 ± 71.7	30.6 ± 53.3	*P* = 0.077
Interval PiB-Neuropsychological exam (days)	71.2 ± 68.7	85.1 ± 70.1	86.9 ± 54.8	60.2 ± 78.8	30.6 ± 53.3	*P* = 0.145

For numerical variables, we indicated the mean ± standard deviation. P-values refer to analysis of Kruskal-Wallis, followed by Mann-Whitney U-tests for *post hoc* group comparisons. Note that between-group comparisons were not possible for categorical variables due to the small sample size.

[a]AD, lvPPA, PCA ≠ MCI ($P < 0.05$); [b]AD, PCA ≠ MCI ($P < 0.05$); [c]lvPPA, PCA ≠ MCI; AD ≠ lvPPA ($P < 0.05$); [d]PCA ≠ AD, lvPPA, MCI ($P < 0.05$).

[e]Missing data for five patients; [f]Missing data for one patient; [g]Missing data for 12 patients.

AD = patients who met McKhann criteria for probable Alzheimer's disease dementia, but did not fulfill criteria for lvPPA or PCA; NA = not applicable; lvPPA = logopenic variant primary progressive aphasia; PCA = posterior cortical atrophy.

disease dementia but did not fulfil criteria for posterior cortical atrophy or logopenic variant primary progressive aphasia (referred as AD group in Table 1) had early age-of-onset Alzheimer's disease (<65 years old; $n = 13/20$), which is often characterized by a mixed clinical presentation, with amnestic and non-amnestic deficits. This heterogeneity is well reflected in the fact that episodic memory was the most impaired cognitive domain in only 10/20 of these patients. All patients had a positive PiB-PET scan, as assessed by visual read according to previously published procedures (Rabinovici *et al.*, 2010), increasing the likelihood of Alzheimer's disease aetiology (McKhann *et al.*, 2011). Furthermore, all patients with CSF data ($n = 18$) presented with a pathological ratio p-tau/amyloid-β_{42} using a previously established threshold (Shaw *et al.*, 2009). Finally, it is worth mentioning that half of the sample (20/40) carried the *APOE* ε4 allele (Table 1). These patients were distributed across the clinical syndromes and did not differ from ε4 non-carriers for demographic features or performance on cognitive domains (Supplementary Table 1).

Neuropsychological tests

Within a maximum of 1 year from the PET scans, the participants underwent a neuropsychological test battery assessing episodic and semantic memory, language, executive and visuospatial functions (Kramer *et al.*, 2003). Episodic memory was assessed using the immediate free recall, delayed (30 s and 10 min) free recall and recognition (10 min) items from the 9-item California Verbal Learning Test and the delayed recall of the Benson figure. Semantic memory was measured using the 15-item Boston Naming Test, 16-item version of the Peabody Picture Vocabulary Test – Revised and category fluency (1 min, animals). Language assessment involved the sentence comprehension subtest from the Curtiss-Yamade Comprehensive Language Evaluation-Receptive, Verbal Agility, and Oral Repetition. Executive functions were evaluated with the Digits Backward from Wechsler Memory Scale, letter (1 min, 'd') and design (1 min) fluencies, modified Trail-Making B and Stroop tests. Finally, the copy trial of the Benson figure and Number Location condition from the Visual Object Spatial Perception battery were used to assess visuospatial abilities.

To obtain composite scores for each cognitive domain, we first used a group of 564 cognitively normal individuals recruited at UCSF [47.3% male, mean age: 67.2 ± 7.1, mean years of education: 17.4 ± 2.0, all with a Mini-Mental State Examination (MMSE) > 27] to convert raw cognitive scores into W-scores (O'Brien and Dyck, 1995) corresponding to Z-scores adjusted for age. Subsequently, patient W-scores were averaged within each cognitive domain (for details on the weight of each cognitive test and score, see Supplementary Table 2). Note that some patients had missing data for certain cognitive tests and that their composite score was therefore computed using remaining scores. Doing so, we were able to compute composite scores of episodic memory and executive functions for all patients (40/40), and scores of semantic memory, language and visuospatial functions for 39/40 patients.

Image acquisition

All patients underwent a structural MRI and both ^{11}C-PiB and ^{18}F-AV-1451 PET scans within an average delay of 51 ± 70 days (^{18}F-AV-1451 and MRI scans: 65 ± 74 days; ^{18}F-AV-1451 and ^{11}C-PiB scans: 27 ± 64 days; ^{11}C-PiB scans and MRI scans: 60 ± 67 days). For MRI, a high-resolution T_1-weighted magnetization prepared rapid gradient echo (MPRAGE) sequence was acquired on a 3 T Siemens Tim Trio scanner at the UCSF Neuroimaging Center (coronal slice orientation; slice thickness = 1.0 mm; in-plane resolution = 1.0 × 1.0 mm; matrix = 240 × 256; repetition

time = 2300 ms; echo time = 2.98 ms; inversion time = 900 ms; flip angle = 9°). PET scans were performed at LBNL on a Siemens Biograph 6 Truepoint PET/CT scanner in 3D acquisition mode. A low-dose CT scan was performed for attenuation correction prior to all scans. ^{11}C-PiB scans were performed as previously described (Lehmann *et al.*, 2013). The ^{18}F-AV-1451 was synthesized and radiolabelled at LBNL's Biomedical Isotope Facility (for details, see Schöll *et al.*, 2016). After injection of ~370 MBq of ^{18}F-AV-1451, PET imaging began either upon injection from 0–100 min and 120–150 min post-injection, or from 75–115 min. For all analyses, we used data reconstructed with ordered subset expectation maximization algorithm (scatter correction, 4 mm Gaussian kernel) and collected from 80–100 min.

Image processing

Neuroimaging data processing was performed using the Statistical Parametric Mapping Version 12 (SPM12) software (Wellcome Department of Imaging Neuroscience, Institute of Neurology, London, England) implemented in MATLAB 8.3. (The MathWorks, Sherborn, MA). T_1-MRI were first segmented and spatially normalized to the MNI space. Grey matter maps were modulated and divided by the total intracranial volume to correct for head size. PET data were realigned and co-registered onto their corresponding MRI. Distribution volume ratios (DVRs) were created for PiB images using Logan graphical analysis (35–90 min post-injection) and a cerebellar grey matter mask (derived from Freesurfer 5.3 segmentation) as reference region. Global cortical ^{11}C-PiB DVR ('global PiB DVR') values were calculated using native space Freesurfer-derived cortical grey matter masks for each participant. The same cerebellar grey matter region was used to compute ^{18}F-AV-1451 standard uptake value ratios (SUVRs). Both ^{11}C-PiB DVR and ^{18}F-AV-1451 SUVR maps were then normalized using the deformation parameters defined from the MRI procedure. As PET and MRI images did not have the same original spatial resolution, a differential Gaussian kernel smoothing was applied to obtain an equivalent data effective smoothing of 8 mm full-width at half-maximum (Chételat *et al.*, 2008). To reduce contamination from non-relevant signal, PET images were masked before smoothing to exclude non-grey and non-white matter voxels (i.e. voxels with a grey or white matter probability lower than 0.25 at the group level).

Informed consent

Informed consent was obtained from all subjects or their assigned surrogate decision-makers, and UCSF, University of California Berkeley, and the Lawrence Berkeley National Laboratory (LBNL) institutional review boards for human research approved the study.

Statistical analysis

First, voxel-wise regressions were performed in SPM to assess the relationship between each imaging modality (i.e. grey matter volume, ^{18}F-AV-1451 SUVR, and ^{11}C-PiB DVR) and each cognitive domain score. These analyses were repeated with age and/or MMSE score as covariates to assess the influence of these variables on the neuroimaging-cognition relationships. We then used the Biological Parametric Mapping (BPM) toolbox to assess voxel-wise relationships between ^{18}F-AV-1451 SUVR and cognitive performance while controlling (in separate models) for (i) local grey matter volume (i.e. maps of grey matter volume entered as a covariate); (ii) local ^{11}C-PiB DVR (i.e. maps of ^{11}C-PiB DVR entered as a covariate); (iii) global ^{11}C-PiB DVR; (iv) local grey matter volume and local ^{11}C-PiB DVR; and (v) local grey matter volume and global ^{11}C-PiB DVR. Given that BPM requires an imaging modality as the dependent variable, we computed a cognitive map for each patient and each cognitive domain by multiplying the binary mask of grey matter (used for the analyses) by the cognitive scores (e.g. the episodic memory map of a given patient contains only one value in all voxels of interest corresponding to that patient's composite episodic memory score). A threshold of $P < 0.001$ uncorrected, together with a cluster extent $k > 500\,mm^3$, was used for all of these neuroimaging analyses.

Finally, partial correlations and causal mediation analyses were performed in the brain regions where cognitive impairment was related to both ^{18}F-AV-1451 SUVR and grey matter volume. These analyses were intentionally restricted to overlap regions in which cognition was found to be correlated with both modalities, in order to avoid a bias for finding a stronger relationship between cognition and one modality as compared to the other. We used the 'mediation' R package (Tingley *et al.*, 2014) to compute the average direct effect (ADE) and average causal mediation effect (ACME), reflecting direct and indirect (i.e. mediated) effects of ^{18}F-AV-1451 on cognitive performance. Both measurements (ACME and ADE) were expressed as a population average estimated using non-parametric bootstrapping (5000 simulations, $P < 0.05$).

Results

Cognitive results

The mean and standard deviation of patient W-scores for each cognitive domain are shown in Table 1. One sample *t*-tests indicated that patient W-scores differed significantly from 0 for all cognitive domains, indicating worse performance relative to controls: episodic memory [$t(39) = -11.6$, $P < 0.001$], semantic memory [$t(38) = -6.5$, $P < 0.001$], language [$t(38) = -5.7$, $P < 0.001$], executive [$t(39) = -12.4$, $P < 0.001$] and visuospatial [$t(38) = -4.8$, $P < 0.001$] functions. The proportion of patients with impaired performance relative to the 95th percentile of controls (W-score < −1.65) was 77.5% for episodic memory, 46.1% for semantic memory, 48.7% for language, 70% for executive functions and 73.6% for visuospatial functions. As expected, patients with MCI were less impaired than those with dementia. Patients meeting criteria for posterior cortical atrophy and logopenic variant primary progressive aphasia showed the greatest impairment in visuospatial and language tests, respectively, while remaining patients with Alzheimer's disease showed greatest impairment as a group in episodic memory (see Table 1 for between-group comparisons).

Relationship between cognition and individual neuroimaging modalities

The results of the independent regressions between cognitive performance and grey matter volume, ^{18}F-AV-1451 SUVR, and ^{11}C-PiB DVR are depicted in Figs 1–3.

Episodic memory performance was associated with decreased grey matter volume in the lateral and medial parietal cortex, left amygdala, left fusiform and middle frontal gyrus, and right middle temporal region. Similarly, the relationship with ^{18}F-AV-1451 encompassed the angular gyrus and medial temporal structures (i.e. entorhinal,

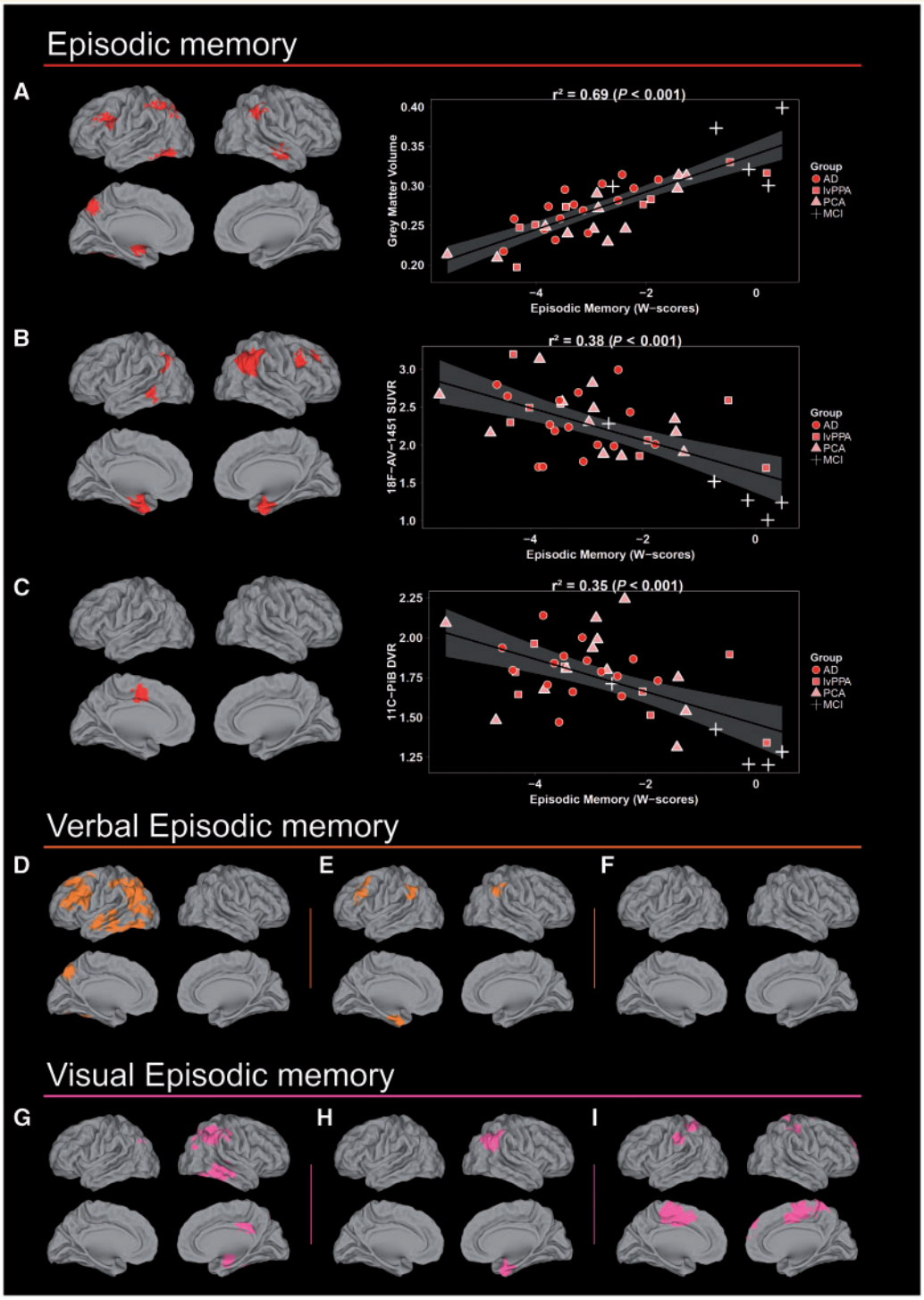

Figure 1 Voxel-wise results of the independent regressions between episodic memory scores and each imaging modality. (**A**, **D** and **G**) Grey matter volume, (**B**, **E** and **H**) ^{18}F-AV-1451 SUVR and (**C**, **F** and **I**) ^{11}C-PiB DVR. Scatterplots and r^2 values were obtained by extracting neuroimaging values from significant clusters. Results are shown in neurologic convention. AD = patients who met McKhann criteria for probable Alzheimer's disease dementia, but did not fulfill criteria for lvPPA or PCA; lvPPA = logopenic variant primary progressive aphasia; PCA = posterior cortical atrophy.

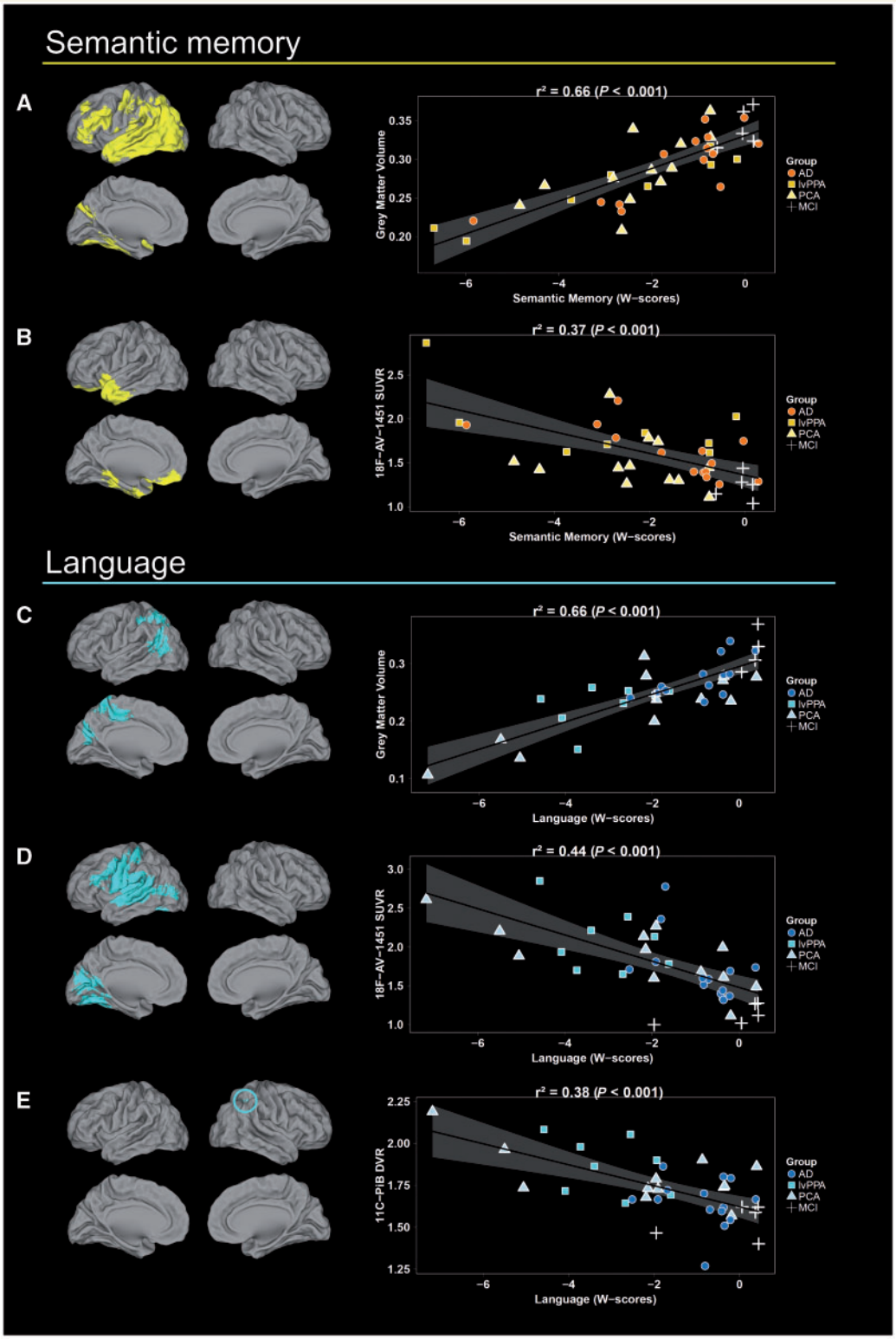

Figure 2 Voxel-wise results of the independent regressions between semantic memory and language scores and each imaging modality. (**A** and **C**) Grey matter volume, (**B** and **D**) ^{18}F-AV-1451 SUVR and (**E**) ^{11}C-PiB DVR. Scatterplots and r^2 values were obtained by extracting neuroimaging values from significant clusters. Note that the relationship between ^{11}C-PiB DVR and semantic memory is not depicted as no significant result was obtained. Results are shown in neurologic convention. AD = patients who met McKhann criteria for probable Alzheimer's disease dementia, but did not fulfill criteria for lvPPA or PCA; lvPPA = logopenic variant primary progressive aphasia; PCA = posterior cortical atrophy.

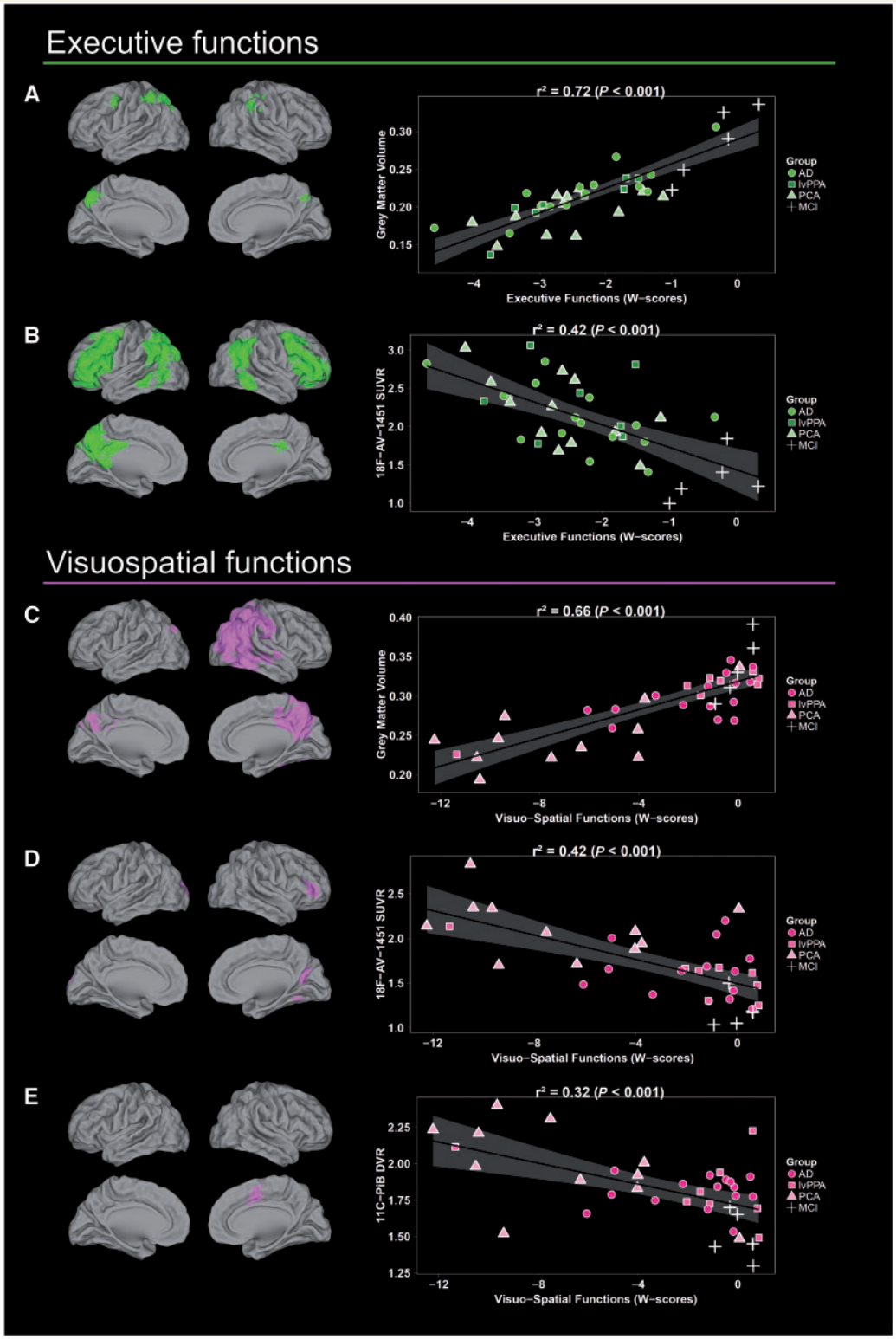

Figure 3 Voxel-wise results of the independent regressions between executive and visuospatial scores and each imaging modality. (**A** and **C**) Grey matter volume, (**B** and **D**) ^{18}F-AV-1451 SUVR and (**E**)^{11}C-PiB DVR. Scatterplots and r^2 values were obtained by extracting neuroimaging values from significant clusters. Note that the relationship between ^{11}C-PiB DVR and executive functions is not depicted as no significant result was obtained. Results are shown in neurologic convention. AD = patients who met McKhann criteria for probable Alzheimer's disease dementia, but did not fulfill criteria for lvPPA or PCA; lvPPA = logopenic variant primary progressive aphasia; PCA = posterior cortical atrophy.

hippocampus and amygdala), left middle temporal and right middle frontal gyri. The regression with ^{11}C-PiB DVR only revealed a significant association in the left supplementary motor area and middle cingulate cortex. Interestingly, when verbal and visual episodic memory were considered separately, the relationships with volume and ^{18}F-AV-1451 SUVR (Fig. 1), but not with ^{11}C-PiB DVR, predominated in the left versus right hemisphere, respectively.

Semantic memory scores were associated with decreased grey matter volume and higher ^{18}F-AV-1451 uptake only in the left hemisphere and mainly in the temporal lobe, but also involving regions of occipital and parietal lobes and inferior frontal gyrus (Fig. 2). Associations with ^{18}F-AV-1451 SUVR were much less widespread and involved the dorsal and ventral temporal pole, orbitofrontal and fusiform regions. No significant relationship was found between semantic memory and ^{11}C-PiB DVR.

The regressions between language and both grey matter volume and ^{18}F-AV-1451 SUVR showed results restricted to the left hemisphere (Fig. 2). The association with grey matter volume involved the posterior middle temporal gyrus, inferior and superior parietal gyrus, precuneus and cuneus. The relationship with ^{18}F-AV-1451 SUVR predominated in the posterior superior temporal and supramarginal gyrus and extended into the postcentral gyrus and posterior insula. Additional correlations were found in lateral and medial occipital cortex. Finally, an association with ^{11}C-PiB DVR was found only in the right inferior parietal lobule.

Executive functions were related to lower grey matter volume and higher ^{18}F-AV-1451 binding in bilateral fronto-parietal regions (Fig. 3). The association with volume encompassed bilateral lateral and medial parietal cortex and left precentral gyrus. Relationships with ^{18}F-AV-1451 were more extended and further involved the angular gyrus and posterior temporal lobe, as well as inferior and middle frontal gyrus. No significant relationship was observed between executive functions and ^{11}C-PiB DVR.

The regression with visuospatial functions revealed significant associations with volume and ^{18}F-AV-1451 uptake in right, more than left, occipital and parietal regions (Fig. 3). Decreased volume in the middle occipital gyrus, lateral (i.e. angular, inferior and superior gyrus) and medial parietal, and posterior temporal regions were related to decreased visuospatial scores. Associations with ^{18}F-AV-1451 involved the left superior occipital gyrus, right calcarine, posterior fusiform gyrus and inferior frontal cortex. The relationships with ^{11}C-PiB DVR were restricted to the right supplementary motor area and middle cingulate cortex.

Complementary analyses with covariates revealed highly similar results when age was regressed out from the statistical models (Supplementary Figs 1–3). In contrast, controlling for disease severity (i.e. MMSE) had more influence on our findings even though several results remained significant with a more restricted spatial extent. This was expected given that all cognitive domains were moderately to highly correlated with MMSE (episodic memory: $r = 0.72$ $P < 0.001$; semantic memory: 0.72 $P < 0.001$; language: $r = 0.45$ $P < 0.005$; executive functions: $r = 0.66$ $P < 0.001$; visuospatial functions: $r = 0.38$ $P < 0.05$).

Finally, note that performance in each cognitive domain was distributed across Alzheimer's disease phenotypes—with the exception of visuospatial functions for which posterior cortical atrophy presented with prominent deficit—and that the association with each imaging modality did not appear driven by one specific syndrome (see scatterplots in Figs 1–3). To confirm this, we repeated the voxel-wise regressions between each imaging modality and cognitive performance after excluding all patients with posterior cortical atrophy and logopenic variant primary progressive aphasia, and found very similar results to those identified in the entire sample (Supplementary Figs 4–6).

Relationship between cognition and tau controlling for volume or amyloid

To assess whether the relationships between cognition and tau remained significant when grey matter volume or amyloid were taken into account, we performed voxel-wise regressions between each cognitive domain and ^{18}F-AV-1451 SUVR controlling for local atrophy and/or local or global ^{11}C-PiB uptake. As illustrated in Fig. 4, most previous results remained essentially the same although less extensive when local atrophy and global ^{11}C-PiB DVR were regressed out. Only findings related to visuospatial functions did not survive the cluster threshold. Similar results were obtained when local rather than global ^{11}C-PiB DVR was used as a covariate (data not shown). To further quantify these changes, we counted in the significant clusters of the regressions between cognition and ^{18}F-AV-1451 SUVR (without covariate) the total number of voxels that remained significant ($P < 0.001$ uncorrected) after the different corrections. The results showed that most clusters maintained a fair number of significant voxels across the different models tested and that the number of significant voxels was more impacted (i) in smaller clusters; (ii) in visuospatial functions as compared to other cognitive domains; and (iii) in the two models including global ^{11}C-PiB DVR index as covariate (Table 2).

Mediation analyses

To further examine whether grey matter volume may mediate the relationship between cognition and tau, we created overlap maps that included voxel clusters that showed significant association between cognitive performance and both ^{18}F-AV-1451 SUVR and grey matter volume (at $P < 0.005$, $k > 500\,mm^3$). The threshold of these analyses was lowered as only a limited number of small clusters was obtained at $P < 0.001$. The mean ^{18}F-AV-1451 SUVR and grey matter volume were then extracted in the overlap

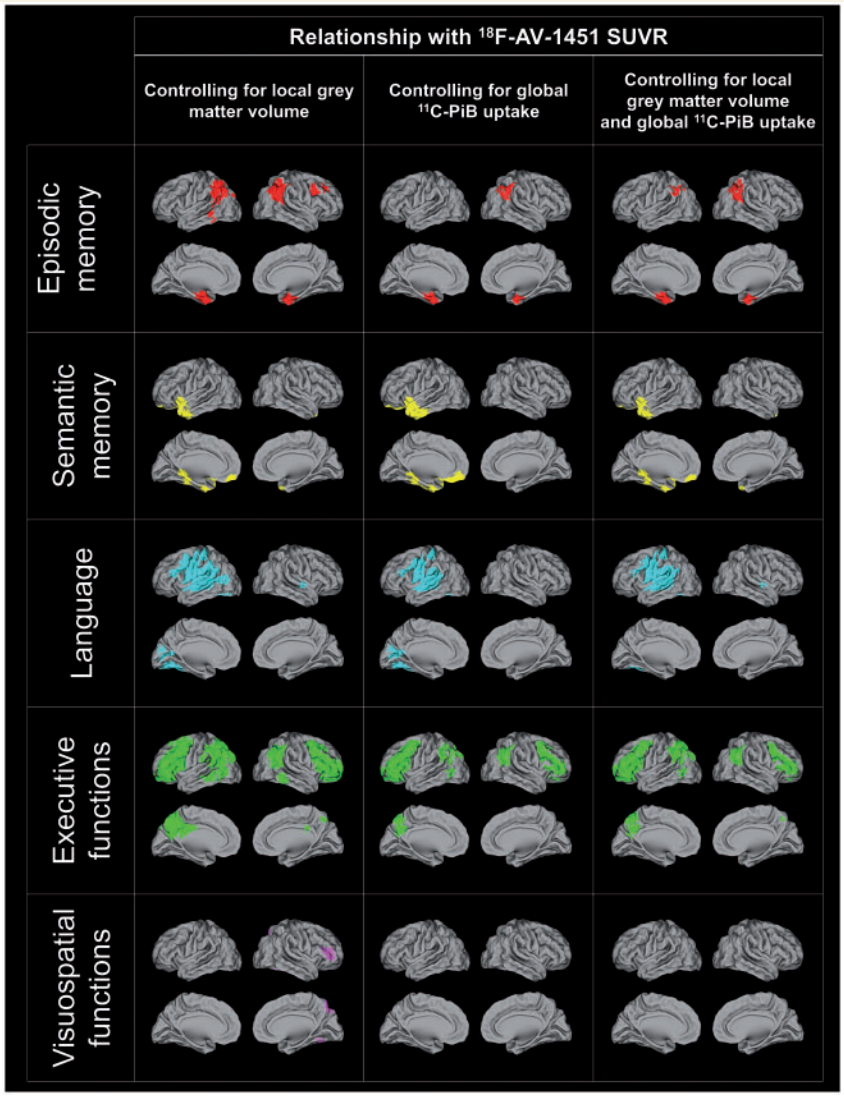

Figure 4 Voxel-wise results of the multiple regressions between ^{18}F-AV-1451 SUVR and each cognitive domain score controlling for local grey matter volume and/or local ^{11}C-PiB DVR. Results are shown in neurologic convention.

regions and used to perform both partial correlations and mediations analyses.

Brain regions in which cognitive domain scores were related to both ^{18}F-AV-1451 SUVR and grey matter volume are displayed in Fig. 5. In these regions, ^{18}F-AV-1451 SUVR was negatively correlated with grey matter volume ($r < -0.4$, $P < 0.05$). Partial correlations showed that the association between ^{18}F-AV-1451 SUVR and episodic memory, language, and executive function scores remained significant when grey matter volume was taken into account. For these cognitive domains, the mediation analyses revealed both direct (i.e. ADE) and atrophy-mediated (i.e. ACME) effects of ^{18}F-AV-1451 SUVR on cognitive performance [note that for episodic memory, the ACME showed a trend toward significance ($P = 0.054$); Fig. 5 and Table 3]. In contrast, only the atrophy-mediated effect (and not the direct effect) was significant for semantic memory and visuospatial functions. Finally, for all cognitive domains, regressions including both ^{18}F-AV-1451 SUVR and grey matter volume explained more variance in the cognitive score (R^2 between 0.41 and 0.73) than ^{18}F-AV-1451 SUVR alone (R^2 between 0.23 and 0.28, Table 3).

Discussion

The recent development of tau PET tracers provided the unique possibility to assess *in vivo* the specific contribution of tau pathology to cognitive impairment in Alzheimer's disease. In the present study, we explored the regional relationships between tau pathology and performance in specific cognitive domains. We further assessed whether these relationships were mediated by neurodegeneration or

Table 2 Spatial extent of the relationship between each cognitive domain and ^{18}F-AV-1451 SUVR with and without controlling for local grey matter atrophy and local or global (mean cortical) ^{11}C-PiB-DVR

Region	Covariates					
	None	GM (local)	PiB-DVR (local)	PiB-DVR (global)	GM (local) and PiB-DVR (local)	GM (local) and PiB-DVR (global)
Episodic memory						
Right lateral parietal cortex	9332	5964 (64)	5606 (60)	2130 (23)	2585 (28)	2028 (22)
Left medial temporal lobe	2271	2082 (92)	1917 (84)	1731 (76)	1789 (79)	1877 (83)
Right medial temporal lobe	1823	1576 (86)	1289 (71)	645 (35)	1094 (60)	888 (49)
Left lateral parietal cortex	1195	1137 (95)	638 (53)	**0 (0)**	641 (54)	176 (15)
Left middle temporal gyrus	834	601 (72)	**0 (0)**	**0 (0)**	**0 (0)**	**0 (0)**
Right middle frontal gyrus	749	648 (87)	351 (47)	41 (5)	297 (40)	149 (20)
Right superior frontal gyrus	530	496 (94)	57 (11)	54 (10)	101 (19)	74 (14)
Semantic memory						
Left anterior temporal cortex	12 164	6602 (54)	12 039 (99)	11 985 (99)	7034 (58)	6456 (53)
Left orbitofrontal cortex	8417	3115 (37)	7239 (86)	8316 (99)	2913 (35)	3078 (37)
Left lingual	3176	2255 (71)	3119 (98)	3122 (98)	2096 (66)	2167 (68)
Language						
Left superior temporal gyrus	37 031	34 010 (92)	27 044 (73)	26 207 (71)	26 919 (73)	29 066 (78)
Left fusiform gyrus/cerebellum	5623	4047 (72)	2255 (40)	3162 (56)	1144 (20)	1779 (32)
Left pericalcarine	2514	1141 (45)	1900 (76)	1313 (52)	581 (23)	486 (19)
Left postcentral gyrus	1721	1630 (95)	915 (53)	1245 (72)	803 (47)	1229 (71)
Executive functions						
Left middle frontal gyrus	45 914	40 973 (89)	34 135 (74)	26 858 (58)	25 326 (55)	24 715 (54)
Left lateral and medial parietal cortex	28 252	24 840 (88)	21 759 (77)	7374 (26)	17 931 (63)	12 086 (43)
Right middle frontal gyrus	23 163	19 784 (85)	11 873 (51)	10 051 (43)	9396 (41)	9430 (41)
Right lateral parietal cortex	13 422	10 439 (78)	6996 (52)	3601 (27)	4604 (34)	3189 (24)
Left inferior temporal gyrus	1384	921 (67)	273 (20)	30 (2)	138 (10)	91 (7)
Left isthmus cingulate	537	486 (91)	182 (34)	273 (51)	125 (23)	226 (42)
Visuospatial functions						
Right cuneus	1080	**0 (0)**	105 (10)	**0 (0)**	**0 (0)**	**0 (0)**
Left superior occipital gyrus	824	314 (38)	722 (88)	172 (21)	236 (29)	**0 (0)**
Right middle frontal gyrus	770	702 (91)	14 (2)	64 (8)	98 (13)	162 (21)
Right lingual/cerebellum	729	658 (90)	729 (100)	213 (29)	692 (95)	105 (14)

Cluster size is indicated in mm^3 and the numbers in parenthesis represent the per cent of voxels from the model without covariates that survived to the additional covariate(s) ($P < 0.001$ uncorrected).
GM = grey matter volume.

amyloid-β plaques, as measured with grey matter volume and ^{11}C-PiB DVR. We found that the association between ^{18}F-AV-1451 and cognition was not—or only slightly—dependent on amyloid-β burden, but was in part mediated by grey matter atrophy. These results suggest that tau pathology may lead to cognitive deficits through a variety of mechanisms, including, but not limited to, grey matter loss.

In our sample, decreased performance in each cognitive domain was related to increased ^{18}F-AV-1451 SUVR in specific brain regions consistent with established brain-behaviour relationships. The AV-1451 tracer preferentially binds to NFTs and demonstrates high affinity to paired helical filaments of tau (Xia *et al.*, 2013; Lowe *et al.*, 2016; Marquié *et al.*, 2017). Hence, our findings fit with neuropathological evidence in Alzheimer's disease that emphasize the importance of the spatial distribution of NFTs in disruption of specific cognitive domains (Mitchell *et al.*, 2002; Guillozet *et al.*, 2003). Our results are consistent with and expand on previous studies showing strong relationships between ^{18}F-AV-1451 uptake and domain-specific cognitive performance in cognitively normal, MCI and Alzheimer's disease individuals (Cho *et al.*, 2016*b*; Ossenkoppele *et al.*, 2016; Schöll *et al.*, 2016) by including a larger and more heterogeneous sample of Alzheimer's disease patients and assessing relationships across a broad spectrum of cognitive domains.

In contrast with ^{18}F-AV-1451, only a few and regionally non-specific relationships were found between ^{11}C-PiB DVR and cognitive deficits. These results further support neuropathological observations that local amyloid-β plaques have only a modest influence on cognitive functioning (Nelson *et al.*, 2012). Converging results from neuropathological and molecular imaging studies are consistent with a model in which amyloid-β pathology primarily plays an

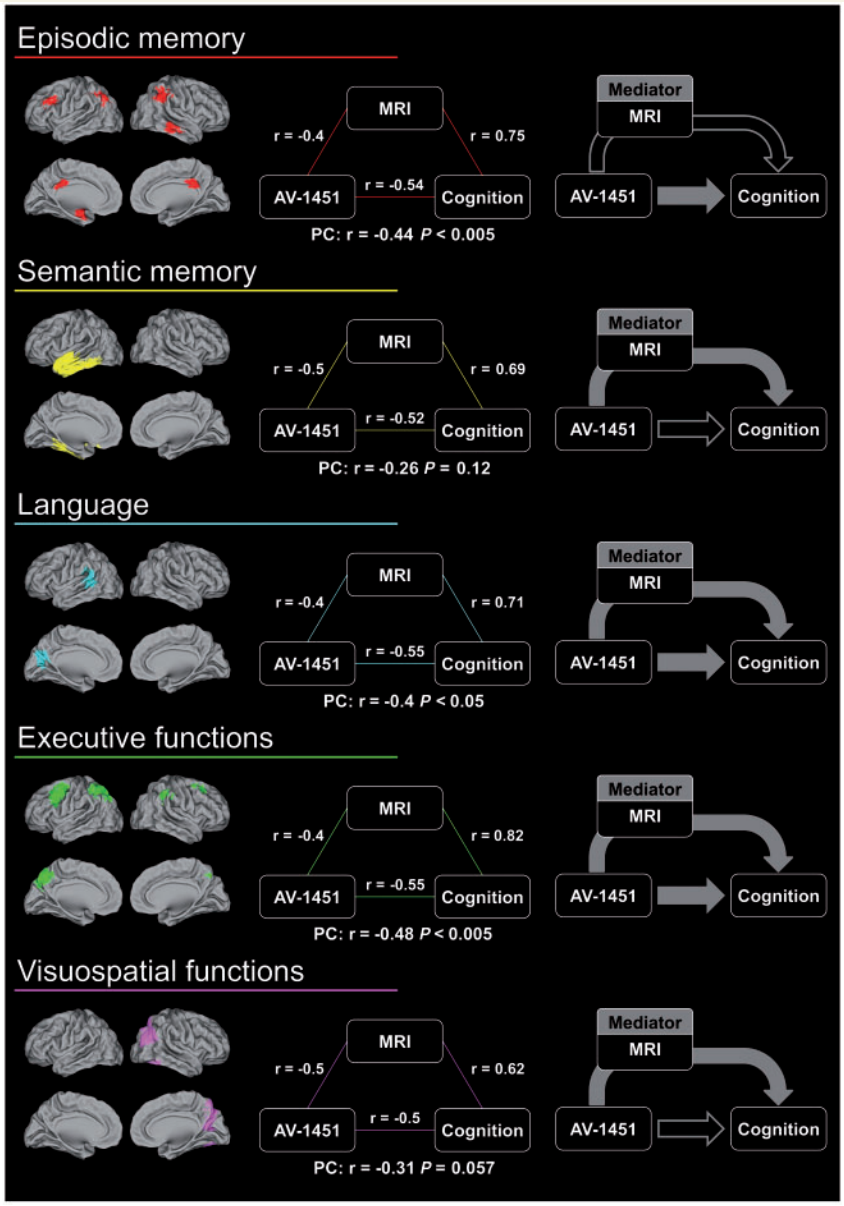

Figure 5 Partial correlations and summary of the mediation analyses in the brain areas where both ^{18}F-AV-1451 SUVR and grey matter volume were related to cognitive domain scores ($P < 0.005$, $k > 500$ mm^3). Filled arrows represent significant effects of the mediation analyses ($P < 0.05$). PC = partial correlation.

Table 3 Mediation analyses and variance explained by ^{18}F-AV-1451 SUVR and grey matter volume for each cognitive domain

	Regressors		Mediation analyses			
			ACME		ADE	
	AV-1451	AV-1451 + GM	Estimates	*P*-values	Estimates	*P*-values
Episodic memory	$r^2 = 0.27$	$r^2 = 0.62$	−0.57 [−1.12/0.01]	0.054	−0.80 [−1.36/−0.16]	0.016
Semantic memory	$r^2 = 0.25$	$r^2 = 0.49$	−1.11 [−2.01/−0.44]	<0.001	−0.80 [−1.72/0.23]	0.122
Language	$r^2 = 0.28$	$r^2 = 0.56$	−0.80 [−1.59/−0.18]	0.003	−1.01 [−1.93/−0.27]	0.007
Executive functions	$r^2 = 0.28$	$r^2 = 0.73$	−0.45 [−0.88/−0.06]	0.021	−0.52 [−0.81/−0.23]	0.001
Visuospatial functions	$r^2 = 0.23$	$r^2 = 0.41$	−1.41 [−2.80/−0.41]	0.002	−1.73 [−3.67/0.27]	0.095

Values in brackets represent 95% confidence interval for the estimates.
ACME = average causal mediation effect; ADE = average direct effect; GM = grey matter volume.

initiating role in early (pre-clinical) stages of the Alzheimer's disease pathophysiological cascade, increasing the severity and rate of accumulation of tau aggregates (Price and Morris, 1999) and promoting tau spread beyond the medial temporal lobe into neocortex (Johnson *et al.*, 2016; Schöll *et al.*, 2016). However, by the time individuals develop clinically apparent cognitive deficits (MCI or dementia), there is an apparent dissociation between the distribution of amyloid and clinical symptoms (Lehmann *et al.*, 2013; Ossenkoppele *et al.*, 2016). Interestingly, we found that global cortical ^{11}C-PiB DVR had a greater impact than local amyloid tracer retention in attenuating the spatial extent of the relationship between tau and cognitive impairment (Table 2). This finding is consistent with previous results showing correlations between global cortical ^{11}C-PiB DVR and ^{18}F-AV-1451 deposition in specific regions (Johnson *et al.*, 2016; Schöll *et al.*, 2016). As previously suggested in neuropathological studies (Giannakopoulos *et al.*, 2003), it may be that global amyloid burden impacts cognition primarily by driving tau pathology in specific brain regions.

Cognitive deficits were also related in a region-specific manner to grey matter loss. The associations between cognition and grey matter or ^{18}F-AV-1451 reflected similar though not entirely overlapping patterns, implicating expected brain regions based on established functional neuroanatomy. Grey matter showed stronger and (in most instances) more spatially extensive relationships with cognitive impairment than ^{18}F-AV-1451. These stronger relations are consistent with the notion that cognitive deficit is most proximally related to grey matter integrity, a hypothesis supported by neuropathological data showing that synaptic density is the strongest predictor of ante-mortem cognition (Terry *et al.*, 1991). The discrepancies between tau and grey matter correlates of cognition may be indicative of the fact that grey matter atrophy is a consequence of diverse neuropathological processes, including tau, amyloid-β, and vascular pathologies (Villeneuve *et al.*, 2015), and likely also represents pre-morbid differences across individuals. Our formal mediation analysis confirmed that grey matter atrophy was a significant mediator of the relationship between tau pathology and cognitive deficits, converging with previous work showing that glucose metabolism measured by ^{18}F-FDG PET, a correlate of synaptic function, mediated the relationship between ^{18}F-THK5317 uptake (i.e. another tau PET radiotracer) and global cognitive impairment in Alzheimer's disease (Saint-Aubert *et al.*, 2016). Our study extends these findings by showing an intermediate role for neurodegeneration using (i) a different tau PET ligand; (ii) a different index of neurodegeneration; and (iii) specific cognitive domains. Interestingly, a longitudinal study also reported that hypometabolism acts as a mediator between CSF tau levels and subsequent cognitive impairment (Dowling *et al.*, 2015). Taken together, these results reinforce the view that tau pathology can lead to neuronal loss and dysfunction, which in turn cause cognitive impairment.

Yet, our results also argue in favour of an independent effect (i.e. neither atrophy- nor amyloid-mediated) of tau pathology on cognition as we found that most regional relationships between ^{18}F-AV-1451 uptake and cognitive impairment remained significant after including grey matter volume and ^{11}C-PiB DVR as covariates in the model. Furthermore, cognitive deficits were related to ^{18}F-AV-1451 uptake but not to atrophy or ^{11}C-PiB binding in certain brain regions and a direct effect of ^{18}F-AV-1451 binding on cognition was identified in the mediation analyses. Given that AV-1451 primarily binds to NFTs (Lowe *et al.*, 2016), our results corroborate neuropathological data indicating that NFTs predict MMSE score independently of neuron numbers and amyloid load (Giannakopoulos *et al.*, 2003; von Gunten *et al.*, 2006). NFTs have historically been considered to play a key role in the pathogenesis of Alzheimer's disease, but growing evidence demonstrated that they are neither necessary nor sufficient for neurodegeneration (Spires-Jones *et al.*, 2011; Cowan and Mudher, 2013). It is nevertheless possible that NFT-bearing neurons present with structural changes that compromise their functioning. In support of this idea, some components involved in the formation of NFTs (i.e. small soluble tau oligomers) may be responsible for tau-induced toxicity (Cowan and Mudher, 2013). Furthermore, in mouse models of tauopathy and human Alzheimer's disease brain, NFT-bearing neurons showed, as compared to non-tangle-bearing neurons, morphometric alterations of Golgi apparatus (Antón-Fernández *et al.*, 2017), lower levels of synaptic proteins (Callahan *et al.*, 1999; Ginsberg *et al.*, 2000) and synaptic reduction (Katsuse *et al.*, 2006). These alterations may impact neuronal function and contribute to cognitive impairment, although discrepant results have been observed (Kuchibhotla *et al.*, 2014).

An alternative explanation is that ^{18}F-AV-1451 SUVR reflects the local severity of tau-pathological processes, as diverse tau species besides NFTs (e.g. ghost tangles, tau neuritic pathology) contribute to AV-1451 binding (Lowe *et al.*, 2016) and strong relationships between distinct pathological species of tau have been reported in human brain tissue (Koss *et al.*, 2016). While the specific tau specie(s) responsible for toxicity remain unclear (Cowan and Mudher, 2013), it has been shown that tau pathology can lead to alterations in synaptic function by disrupting cellular trafficking pre- and postsynaptically and inhibiting anterograde axonal transport (Spires-Jones and Hyman, 2014). As a result, pathological tau can reduce the activity of neurons in transgenic mice and possibly cause network disruption prior to substantial neurodegeneration (Menkes-Caspi *et al.*, 2015). We therefore hypothesize that tau-mediated synaptic abnormalities may trigger local neuronal dysfunction, which in turn induces cognitive deficits prior to neuronal death. Further studies are necessary to confirm this pathological cascade and to assess whether tau-mediated synaptic disruption emerges before versus with grey matter loss. Alternatively, ^{18}F-AV-1451 uptake may

better reflect the neurodegenerative process related to tau pathology than volumetric measurement. Indeed, due to their high pre-morbid variability across individuals, cross-sectional measures of grey matter volume may be less sensitive to the local tau-mediated neurodegeneration than ^{18}F-AV-1451.

Our study has limitations. First, causal relationships between grey matter atrophy, ^{18}F-AV-1451, and ^{11}C-PiB DVR uptake could not be assessed due to the cross-sectional and correlational nature of this study. Longitudinal investigations will be critical to further specify the associations between these biomarkers and characterize their relation with cognitive decline. Second, while our population included a total of 40 patients, the sample size of some clinical subgroups (e.g. MCI or logopenic variant primary progressive aphasia) was relatively small. Furthermore, our sample included patients with diverse and less common Alzheimer's disease phenotypes, which may have driven correlations in specific domains (e.g. visuospatial deficits in posterior cortical atrophy). Reassuringly, examination of individual data points suggests that contributions to domain-specific correlations were distributed across Alzheimer's disease phenotypes, with prominent visuospatial deficits in posterior cortical atrophy being the one exception. Furthermore, our results include strong correlations with cognitive domains that are not uniquely or disproportionately impacted in any individual Alzheimer's disease clinical variant, and results were relatively consistent after exclusion of patients with posterior cortical atrophy and logopenic variant primary progressive aphasia. Conversely, the inclusion of a diverse Alzheimer's disease clinical sample enriched our cohort for heterogeneity in cognition, AV-1451 and grey matter atrophy patterns, increasing our ability to detect meaningful associations. Finally, one may argue that analysing ^{18}F-AV-1451 data collected from 80–100 min post-injection may underestimate the SUVR values in structures with a high binding (Baker *et al.*, 2017) and therefore alter some relationships with cognitive performance. However, this time window also appears to be the best selection for studying the full range of tau deposition (Baker *et al.*, 2017) and therefore represents a good compromise for whole brain analyses.

In summary, our study demonstrated intimate relationships between local tau pathology and domain-specific cognitive impairment in symptomatic Alzheimer's disease. In agreement with a causal sequence of pathological events, grey matter atrophy was shown to play an intermediary role in these relationships. However, we also provide novel evidence that tau pathology may contribute to cognitive deficits independent of grey matter loss. These results suggest that cognitive impairment results from diverse tau-mediated pathological processes in Alzheimer's disease, which has implications for future therapeutic trials targeting tau pathology.

Acknowledgements

We thank K. Norton, S.N. Lockhart, L. Kritikos and R. Kettele for their technical and administrative support, and E. M. Arenaza-Urquijo for her scientific inputs. Avid Radiopharmaceuticals enabled the use of the ^{18}F-AV-1451 tracer by providing precursor, but did not provide direct funding and was not involved in data analysis or interpretation.

Funding

This research was funded by Fondation pour la Recherche Medicale (to A.B.), National Institute on Aging grants (R01-AG045611; to G.D.R.), (R01-AG034570; to W.J.J.), (P50-AG023501; to B.L.M and G.D.R.), (P01-AG019724; to M.G.), (U01-AG052943; to M.G.); National Institute of Neurological Disorders and Stroke (R01-NS050915; to M.G.), (K24-DC015544; to M.G.); Tau Consortium (to G.D.R. and W.J.J); State of California Department of Health Services Alzheimer's Disease Research Centre of California grant (04-33516; to B.L.M); John Douglas French Alzheimer's Foundation (to G.D.R. and B.L.M.).

Conflicts of interest

G.D.R. receives research support from Avid Radiopharmaceuticals/Eli Lilly, GE Healthcare and Piramal. He has received speaking honoraria or consulting fees from Eisai, Genentech, Lundbeck, Merck, Putnam, Roche. W.J.J. is a consultant for Genentech, Novartis, and Bioclinica. B.L.M.: Medical Director for John Douglas French Foundation; Scientific Director for the Tau Consortium; Director/Medical Advisory Board of the Larry L. Hillblom Foundation; Scientific Advisory Board Member for the National Institute for Health Research Cambridge Biomedical Research Centre and its subunit, the Biomedical Research Unit in Dementia (UK); and Board Member for the American Brain Foundation (ABF).

Supplementary material

Supplementary material is available at *Brain* online.

References

Albert MS, DeKosky ST, Dickson D, Dubois B, Feldman HH, Fox NC, et al. The diagnosis of mild cognitive impairment due to Alzheimer's disease: recommendations from the National Institute on Aging-Alzheimer's Association workgroups on diagnostic guidelines for Alzheimer's disease. Alzheimers Dement 2011; 7: 270–9.

Antón-Fernández A, Aparicio-Torres G, Tapia S, DeFelipe J, Muñoz A. Morphometric alterations of Golgi apparatus in Alzheimer's

disease are related to tau hyperphosphorylation. Neurobiol Dis 2017; 97: 11–23.
Arriagada PV, Growdon JH, Hedley-Whyte ET, Hyman BT. Neurofibrillary tangles but not senile plaques parallel duration and severity of Alzheimer's disease. Neurology 1992a; 42: 631–9.
Arriagada PV, Marzloff K, Hyman BT. Distribution of Alzheimer-type pathologic changes in nondemented elderly individuals matches the pattern in Alzheimer's disease. Neurology 1992b; 42: 1681–8.
Baker SL, Lockhart SN, Price JC, He M, Huesman RH, Schonhaut D, et al. Reference tissue-based kinetic evaluation of 18F-AV-1451 for tau imaging. J Nucl Med 2017; 58: 332–8.
Braak H, Del Tredici K. The preclinical phase of the pathological process underlying sporadic Alzheimer's disease. Brain 2015; 138: 2814–33.
Callahan LM, Vaules WA, Coleman PD. Quantitative decrease in synaptophysin message expression and increase in cathepsin D message expression in Alzheimer disease neurons containing neurofibrillary tangles. J Neuropathol Exp Neurol 1999; 58: 275–87.
Chételat G, Desgranges B, Landeau B, Mézenge F, Poline JB, de la Sayette V, et al. Direct voxel-based comparison between grey matter hypometabolism and atrophy in Alzheimer's disease. Brain 2008; 131: 60–71.
Cho H, Choi JY, Hwang MS, Kim YJ, Lee HM, Lee HS, et al. *In vivo* cortical spreading pattern of tau and amyloid in the Alzheimer disease spectrum. Ann Neurol 2016a; 80: 247–58.
Cho H, Choi JY, Hwang MS, Lee JH, Kim YJ, Lee HM, et al. Tau PET in Alzheimer disease and mild cognitive impairment. Neurology 2016b; 87: 375–83.
Cowan CM, Mudher A. Are tau aggregates toxic or protective in tauopathies? Front Neurol 2013; 4: 114.
Dowling NM, Johnson SC, Gleason CE, Jagust WJ, Alzheimer's Disease Neuroimaging Initiative. The mediational effects of FDG hypometabolism on the association between cerebrospinal fluid biomarkers and neurocognitive function. Neuroimage 2015; 105: 357–68.
Dronse J, Fliessbach K, Bischof GN, von Reutern B, Faber J, Hammes J, et al. *In vivo* patterns of tau pathology, amyloid-β burden, and neuronal dysfunction in clinical variants of Alzheimer's disease. J Alzheimers Dis 2016; 55: 465–71.
Dubois B, Feldman HH, Jacova C, Hampel H, Molinuevo JL, Blennow K, et al. Advancing research diagnostic criteria for Alzheimer's disease: the IWG-2 criteria. Lancet Neurol 2014; 13: 614–29.
Gefen T, Gasho K, Rademaker A, Lalehzari M, Weintraub S, Rogalski E, et al. Clinically concordant variations of Alzheimer pathology in aphasic versus amnestic dementia. Brain 2012; 135: 1554–65.
Giannakopoulos P, Herrmann FR, Bussière T, Bouras C, Kövari E, Perl DP, et al. Tangle and neuron numbers, but not amyloid load, predict cognitive status in Alzheimer's disease. Neurology 2003; 60: 1495–500.
Ginsberg SD, Hemby SE, Lee VM, Eberwine JH, Trojanowski JQ. Expression profile of transcripts in Alzheimer's disease tangle-bearing CA1 neurons. Ann Neurol 2000; 48: 77–87.
Gómez-Isla T, Hollister R, West H, Mui S, Growdon JH, Petersen RC, et al. Neuronal loss correlates with but exceeds neurofibrillary tangles in Alzheimer's disease. Ann Neurol 1997; 41: 17–24.
Gorno-Tempini ML, Hillis AE, Weintraub S, Kertesz A, Mendez M, Cappa SF, et al. Classification of primary progressive aphasia and its variants. Neurology 2011; 76: 1006–14.
Guillozet AL, Weintraub S, Mash DC, Mesulam MM. Neurofibrillary tangles, amyloid, and memory in aging and mild cognitive impairment. Arch Neurol 2003; 60: 729–36.
Hof PR, Bouras C, Constantinidis J, Morrison JH. Balint's syndrome in Alzheimer's disease: specific disruption of the occipito-parietal visual pathway. Brain Res 1989; 493: 368–75.
Hyman BT, Phelps CH, Beach TG, Bigio EH, Cairns NJ, Carrillo MC, et al. National Institute on Aging-Alzheimer's Association guidelines for the neuropathologic assessment of Alzheimer's disease. Alzheimers Dement 2012; 8: 1–13.
Jack CR, Dickson DW, Parisi JE, Xu YC, Cha RH, O'Brien PC, et al. Antemortem MRI findings correlate with hippocampal neuropathology in typical aging and dementia. Neurology 2002; 58: 750–7.
Johnson KA, Schultz A, Betensky RA, Becker JA, Sepulcre J, Rentz D, et al. Tau positron emission tomographic imaging in aging and early Alzheimer disease. Ann Neurol 2016; 79: 110–19.
Katsuse O, Lin W-L, Lewis J, Hutton ML, Dickson DW. Neurofibrillary tangle-related synaptic alterations of spinal motor neurons of P301L tau transgenic mice. Neurosci Lett 2006; 409: 95–9.
Koss DJ, Jones G, Cranston A, Gardner H, Kanaan NM, Platt B. Soluble pre-fibrillar tau and β-amyloid species emerge in early human Alzheimer's disease and track disease progression and cognitive decline. Acta Neuropathol 2016; 132: 875–95.
Kramer JH, Jurik J, Sha SJ, Rankin KP, Rosen HJ, Johnson JK, et al. Distinctive neuropsychological patterns in frontotemporal dementia, semantic dementia, and Alzheimer disease. Cogn Behav Neurol 2003; 16: 211–18.
Kuchibhotla KV, Wegmann S, Kopeikina KJ, Hawkes J, Rudinskiy N, Andermann ML, et al. Neurofibrillary tangle-bearing neurons are functionally integrated in cortical circuits *in vivo*. Proc Natl Acad Sci USA 2014; 111: 510–14.
Lehmann M, Ghosh PM, Madison C, Laforce R, Jr, Corbetta-Rastelli C, Weiner MW, et al. Diverging patterns of amyloid deposition and hypometabolism in clinical variants of probable Alzheimer's disease. Brain 2013; 136: 844–58.
Lowe VJ, Curran G, Fang P, Liesinger AM, Josephs KA, Parisi JE, et al. An autoradiographic evaluation of AV-1451 Tau PET in dementia. Acta Neuropathol Commun 2016; 4: 58.
Marquié M, Siao Tick Chong M, Antón-Fernández A, Verwer EE, Sáez-Calveras N, Meltzer AC, et al. [F-18]-AV-1451 binding correlates with postmortem neurofibrillary tangle Braak staging. Acta Neuropathol 2017; 134: 619–28.
McKhann GM, Knopman DS, Chertkow H, Hyman BT, Jack CR, Jr, Kawas CH, et al. The diagnosis of dementia due to Alzheimer's disease: recommendations from the National Institute on Aging-Alzheimer's Association workgroups on diagnostic guidelines for Alzheimer's disease. Alzheimers Dement 2011; 7: 263–9.
Mendez MF, Ghajarania M, Perryman KM. Posterior cortical atrophy: clinical characteristics and differences compared to Alzheimer's disease. Dement Geriatr Cogn Disord 2002; 14: 33–40.
Menkes-Caspi N, Yamin HG, Kellner V, Spires-Jones TL, Cohen D, Stern EA. Pathological tau disrupts ongoing network activity. Neuron 2015; 85: 959–66.
Mitchell TW, Mufson EJ, Schneider JA, Cochran EJ, Nissanov J, Han L-Y, et al. Parahippocampal tau pathology in healthy aging, mild cognitive impairment, and early Alzheimer's disease. Ann Neurol 2002; 51: 182–9.
Murray ME, Graff-Radford NR, Ross OA, Petersen RC, Duara R, Dickson DW. Neuropathologically defined subtypes of Alzheimer's disease with distinct clinical characteristics: a retrospective study. Lancet Neurol 2011; 10: 785–96.
Nelson PT, Alafuzoff I, Bigio EH, Bouras C, Braak H, Cairns NJ, et al. Correlation of Alzheimer disease neuropathologic changes with cognitive status: a review of the literature. J Neuropathol Exp Neurol 2012; 71: 362–81.
O'Brien PC, Dyck PJ. Procedures for setting normal values. Neurology 1995; 45: 17–23.
Ossenkoppele R, Schonhaut DR, Schöll M, Lockhart SN, Ayakta N, Baker SL, et al. Tau PET patterns mirror clinical and neuroanatomical variability in Alzheimer's disease. Brain 2016; 139: 1551–67.
Price JL, Morris JC. Tangles and plaques in nondemented aging and 'preclinical' Alzheimer's disease. Ann Neurol 1999; 45: 358–68.
Rabinovici GD, Furst AJ, Alkalay A, Racine CA, O'Neil JP, Janabi M, et al. Increased metabolic vulnerability in early-onset Alzheimer's disease is not related to amyloid burden. Brain 2010; 133: 512–28.

Saint-Aubert L, Almkvist O, Chiotis K, Almeida R, Wall A, Nordberg A. Regional tau deposition measured by [(18)F]THK5317 positron emission tomography is associated to cognition via glucose metabolism in Alzheimer's disease. Alzheimers Res Ther 2016; 8: 38.

Salloway S, Sperling R, Fox NC, Blennow K, Klunk W, Raskind M, et al. Two phase 3 trials of bapineuzumab in mild-to-moderate Alzheimer's disease. N Engl J Med 2014; 370: 322–33.

Schöll M, Lockhart SN, Schonhaut DR, O'Neil JP, Janabi M, Ossenkoppele R, et al. PET Imaging of Tau Deposition in the Aging Human Brain. Neuron 2016; 89: 971–82.

Shaw LM, Vanderstichele H, Knapik-Czajka M, Clark CM, Aisen PS, Petersen RC, et al. Cerebrospinal fluid biomarker signature in Alzheimer's disease neuroimaging initiative subjects. Ann Neurol 2009; 65: 403–13.

Spires-Jones TL, Hyman BT. The intersection of amyloid beta and tau at synapses in Alzheimer's disease. Neuron 2014; 82: 756–71.

Spires-Jones TL, Kopeikina KJ, Koffie RM, de Calignon A, Hyman BT. Are tangles as toxic as they look? J Mol Neurosci 2011; 45: 438–44.

Terry RD, Masliah E, Salmon DP, Butters N, DeTeresa R, Hill R, et al. Physical basis of cognitive alterations in Alzheimer's disease: synapse loss is the major correlate of cognitive impairment. Ann Neurol 1991; 30: 572–80.

Tingley D, Yamamoto T, Hirose K, Keele L, Imai K. Mediation: R package for causal mediation analysis [Internet]. J Stat Softw 2014; 59. Available from: https://dspace.mit.edu/handle/1721.1/91154 (7 February 2017, date last accessed).

Villeneuve S, Wirth M, La Joie R. Are AD-typical regions the convergence point of multiple pathologies? Front Aging Neurosci 2015; 7: 42.

von Gunten A, Kövari E, Bussière T, Rivara C-B, Gold G, Bouras C, et al. Cognitive impact of neuronal pathology in the entorhinal cortex and CA1 field in Alzheimer's disease. Neurobiol Aging 2006; 27: 270–7.

Whitwell JL, Josephs KA, Murray ME, Kantarci K, Przybelski SA, Weigand SD, et al. MRI correlates of neurofibrillary tangle pathology at autopsy: a voxel-based morphometry study. Neurology 2008; 71: 743–9.

Xia C-F, Arteaga J, Chen G, Gangadharmath U, Gomez LF, Kasi D, et al. [(18)F]T807, a novel tau positron emission tomography imaging agent for Alzheimer's disease. Alzheimers Dement 2013; 9: 666–76.